Endothelial and hematopoietic hPSCs differentiation via an hematoendothelial progenitor.

Alejandra Vargas-Valderrama
INSERM UMRS-MD 1197, Université Paris-Saclay, Hopital Paul Brousse

Anne-Charlotte Ponsen
INSERM UMRS-MD 1197, Université Paris-Saclay, Hopital Paul Brousse

Estelle Oberlin
INSERM UMRS-MD 1197, Université Paris-Saclay, Hopital Paul Brousse

Morgane Le Gall
INSERM U477: Institut Cochin, INSERM U1016, CNRS UMR8104

Denis Clay
INSERM UMS-44, Université Paris-Saclay, Hopital Paul Brousse

Sébastien Jacques
Plateforme de Génomique-GENOMI'IC, Université de Paris, Institut Cochin, INSERM U1016, CNRS UMR 8104

Tudor Manoliu
Gustave Roussy, Université Paris-Saclay, Plate-forme Imagerie et Cytometrie, UMS AMMICa

Valérie Rouffiac
Gustave Roussy, Université Paris-Saclay, Plate-forme Imagerie et Cytometrie, UMS AMMICa

Karine Ser-le-Roux
INSERM, Gustave Roussy, Plate-forme d'Evaluation Preclinique, UMS AMMICa

Cyril Quivoron
Laboratoire d'Hématologie Tanslationnelle, Gustave Roussy

Fawzia Louache
INSERM UMRS-MD 1197, Université Paris-Saclay, Hopital Paul Brousse

Georges Uzan
INSERM UMRS-MD 1197, Université Paris-Saclay, Hopital Paul Brousse

Hind Guenou
INSERM UMRS-MD 1197, Université Evry-Val-d'Essone, Université Université Paris-Saclay, Hopital Paul Brousse

Maria Teresa Mitjavila-Garcia (maite.mitjavila@inserm.fr)
INSERM UMRS-MD 1197, Université Paris-Saclay, Hopital Paul Brousse https://orcid.org/0000-0002-3995-2266

Research Article

Keywords: Hemogenic endothelium, endothelium, hematopoietic cells, hPSC, hESCs, hiPSC, endothelial differentiation, hematopoietic differentiation.

Posted Date: March 23rd, 2022

DOI: https://doi.org/10.21203/rs.3.rs-1457912/v1

Abstract

Background: hPSC-derived endothelial and hematopoietic cells (ECs and HCs) are an interesting source of cells for tissue engineering. Despite their close spatial and temporal embryonic development, current hPSC differentiation protocols are specialized in only one of these lineages. In this study, we generated a hematoendothelial population that could be further differentiated *in vitro* to both lineages.

Methods: Two hESCs and one hiPSC lines were differentiated into a hematoendothelial population, hPSC-ECs and blast colonies (hPSC-BCs) *via* $CD144^+$-embryoid bodies (hPSC-EBs). hPSC-ECs were characterized by endothelial colony forming assay, LDL uptake assay, endothelial activation by TNF-α, Nitric Oxyde detection and Matrigel-based tube formation. Hematopoietic colony forming cell assay was performed from hPSC-BCs. Interestingly, we identified a hPSC-BC population characterized by the expression of both CD144 and CD45. hPSC-ECs and hPSC-BCs were analyzed by flow cytometry and RT-qPCR, *in vivo* experiments have been realized by ischemic tissue injury model on a mouse dorsal skinfold chamber and hematopoietic reconstitution in irradiated immunosuppressed mouse from hPSC-ECs and hPSC-EB-$CD144^+$ respectively. Transcriptomic analyses were performed to confirm the endothelial and hematopoietic identity of hESC-derived cell populations by comparing them against undifferentiated hESC, among each other's (*e.g.,* hPSC-ECs vs hPSC-EB-$CD144^+$) and against human embryonic liver (EL) endothelial, hematoendothelial and hematopoietic cell sub populations.

Results: A hematoendothelial population was obtained after 84 hours of hPSC-EBs formation under serum-free conditions and isolated based on CD144 expression. Intrafemorally injection of hPSC-EB-$CD144^+$ contributed to the generation of $CD45^+$ human cells in immunodeficient mice suggesting the existence of hemogenic ECs within hPSC-EB-$CD144^+$. Endothelial differentiation of hPSC-EB-$CD144^+$ yields a population of >95% functional ECs *in vitro*. hPSC-ECs derived through this protocol participated at the formation of new vessels *in vivo* in a mouse ischemia model. *In vitro*, hematopoietic differentiation of hPSC-EB-$CD144^+$ generated an intermediate population of >90% $CD43^+$ hPSC-BCs capable to generate myeloid and erythroid colonies. Finally, the transcriptomic analyses confirmed the hematoendothelial, endothelial and hematopoietic identity of hPSC-EB-$CD144^+$, hPSC-ECs and hPSC-BCs, respectively, and the similarities between hPSC-BC-$CD144^+CD45^+$, a subpopulation of hPSC-BCs, and human EL hematopoietic stem cells/hematopoietic progenitors.

Conclusion: The present work reports a hPSC differentiation protocol into functional hematopoietic and endothelial cells through a hematoendothelial population. Both lineages were proven to display characteristics of physiological human cells and therefore, they represent an interesting rapid source of cells for future cell therapy and tissue engineering.

Introduction

The rise of applied biology areas such as tissue engineering and biomedicine has highlighted the importance of endothelial (ECs) and hematopoietic cells (HCs) in building up the complexity of *in vitro*

biological systems. ECs line the walls of blood and lymphatic vessels, assuring the transport of oxygen, nutrients, and cells throughout the human body. HCs encompass a large number of cells ranging from red blood to immune cells. The discovery of human embryonic stem cells (hESCs) (1) and later, the reprogramming of somatic cells into human induced pluripotent stem cells (hiPSCs) (2, 3), opened the possibility to generate *in vitro* large numbers of these and other cell lineages sharing the same genetic background. However, the differentiation of human pluripotent stem cells (hPSCs) into ECs and HCs has been hampered by the limited knowledge on the human embryonic development of both lineages.

Several studies, performed *in vitro* and *in vivo* in animal models such as birds, fish and mice, have now demonstrated the embryonic endothelial origin of adult HSC (4, 5). ECs emerge early during embryonic development from extra- and intra-embryonic mesodermal progenitors. They organize into networks giving place to vascular plexuses and major blood vessels (6). A subpopulation of ECs, known as hemogenic endothelium, located principally at the aorta-gonad-mesonephros (AGM) region but also in the placenta and the yolk sac has been described to undergo endothelial to hematopoietic transition to give rise to primitive and definitive hematopoiesis (7, 8). Hematopoietic progenitors (HP), arising from the hemogenic endothelium and known as pre-hematopoietic stem cells (pre-HSC), display a dual endo-hematopoietic phenotype characterized by the expression of the endothelial-specific junctional vascular endothelial cadherin (Cdh5, CD144) and the presence of the pan-leukocyte antigen CD45 (9–13). They migrate to the fetal liver to expand and maturate before colonizing the bone marrow (BM), the definitive hematopoietic reservoir in adult organisms (14–16). There, ECs keep playing an important role in controlling proliferation and differentiation of HSCs (17).

Despite these close developmental and functional relationship between ECs and HCs, most of the current differentiation protocols of hPSCs focus on the derivation on one of these lineages (5, 18–35). Other authors differentiated both lineages (ECs and HCs) (36, 37). In several studies, hematopoietic progenitors emerged from a hemogenic endothelium differentiated from hPSCs (5, 21, 38–40). ECs and HCs simultaneous differentiation may be beneficial for their maturation and further biomedical applications. In this study, we differentiated hPSCs into well-characterized hematoendothelial progenitors. This population was proven to contain not only endothelial progenitors but also hemogenic ECs that generated HCs *in vitro* through the formation of blast colonies (hPSC-BCs) and *in vivo* in irradiated immunodeficient mice. Similarly, hPSC-ECs derived from this population showed a functional endothelial phenotype *in vitro* and *in vivo* in an ischemia murine model. Finally, we compared at the transcriptional level the different hPSC-derived populations generated with this protocol to EL-ECs, EL-pre-HSCs, EL-HPs/HSCs and mature EL-HCs isolated from human embryonic livers (EL) confirming their endothelial, hematoendothelial and hematopoietic identity.

Materials And Methods

Human pluripotent stem cells

hESCs, SA01 (Cellartis AB, Sweden) and H1 (WiCell Research Institute, USA), were provided by the INSERM cell bank « *ESteam Paris Sud - Plate-forme cellules souches* » (INSERM U935) according to the agreement n° RE14_007R of the French Biomedical Agency. The hiPSC line A29 was derived, characterized, and kindly provided by the team INSERM U1193 led by Dr. Dubart-Kupperschmitt (41). Mitomycin-treated mouse embryonic fibroblasts were used as feeder cells for all hPSCs in Knockout DMEM medium (Gibco) supplemented with 20% Knockout serum replacement (Gibco), 1% penicillin/streptomycin, 1 mM L-glutamine, 1% non-essential amino acids, 0.1 mM β-Mercaptoethanol (all from Gibco) and 5 ng/mL basic fibroblast growth factor (bFGF, Miltenyi) at 37°C and 5% CO_2. The medium was daily replaced by fresh medium and cells were enzymatically passaged upon confluency, by using collagenase type IV at 1 mg/mL (Gibco).

hPSCs differentiation into a hematoendothelial population, hPSC-ECs and hPSC-BCs

Confluent hPSCs, between passages 52 to 100, were enzymatically passaged as described in the preceding paragraph. Small cell clumps were cultured in embryoid body (hPSC-EB) basal medium (Stemline II Hematopoietic Stem Cell Expansion Medium (Sigma-Aldrich) supplied with 1% streptomycin, 1 mM de L-glutamine) supplemented with 50 ng/mL VEGF-A_{165} (Peprotech), 50 ng/mL BMP-4 and 6µM CHIR99021 (StemCell Technologies) in low-attachment culture plates (NUNC, ThermoFisher) at a cellular density equivalent to 3.5 x10^4 cells/ml. After 48h, EB basal medium was refreshed and supplemented with 50 ng/mL of VEGF-A_{165} and BMP-4, and 20 ng/mL of SCF, Flt-3L and TPO (all from Peprotech). At 84h of EB differentiation, EBs were recovered and dissociated enzymatically with Accutase (Corning). $CD144^{+-}$cells were isolated from hPSC-EBs by magnetic-based cell sorting (MACS) using microbeads conjugated with anti-hCD144 antibodies (Miltenyi) on MS sorting columns (Miltenyi) according to the manufacturer's instructions.

$CD144^+$ and $CD144^-$ sorted cells from 84h-hPSC-EBs (Table 1) were plated on fibronectin (Sigma-Aldrich) pre-coated well plates or Lab-Tek chamber slides (ThermoFisher) at a density of 15000 cells/cm^2 in EC culture medium: STEMdiff™ APEL™2 Medium (StemCell Technologies) supplied with 5% FBS (Lonza), 1 mM de L-glutamine, 50 ng/mL VEGF-A_{165} and 10 ng/mL bFGF. 10 µM of DAPT (Sigma Aldrich) was added to the EC culture medium for artery/vein differentiation experiments. hPSC-ECs (Table 1) were cultured at 37°C and 5% CO_2. Medium was replaced every other day. Confluent endothelial cells were passaged enzymatically with Accutase (approximately every 4–6 days).

In order to obtain hPSC-BC (Table 1), 50000 $CD144^+$ and hPSC-EB-$CD144^-$ cells/mL were cultured for 6 days in a serum-free enriched methylcellulose (StemCell Technologies) and EB basal medium supplied with 50 ng/mL of VEGF-A_{165}, BMP-4, TPO and Flt-3L, 20 ng/mL of bFGF and 3 units/mL of EPO in low-attachment culture plates.

Table 1
Undifferentiated and differentiated hPSC populations.

Undifferentiated hPSCs	
Population	**Abbreviation/ Identification used in the text**
hESCs	H1 and SA01 cell lines
hiPSCs	A29
Differentiated hPSCs	
Non-sorted EBs at 84h of differentiation	hPSC-EBs
Sorted EBs based on the expression of CD144	hPSC-EB-CD144^{+}
ECs derived from hPSC-EB-CD144^{+}	hPSC-ECs
BCs derived from hPSC-EB-CD144^{+}	hPSC-BCs
Sorted hPSC-BCs based on the expression of CD144 and CD45	hPSC-BC-CD144^{+}CD45^{+}

Endothelial colony forming assay

Dissociated hPSC-EBs were incubated with fluorochrome-conjugated mouse antibody anti-human CD144 (Miltenyi, clone REA199) for 30 minutes at 4°C. Cells were washed and resuspended in PBS containing 5% FBS and 1µg/mL of 7AAD (Sigma Aldrich). 7AAD^{-}hPSC-EB-CD144^{+} cells were sorted with the BD FacsAria Sorter (BD Biosciences) and plated at 1 cell/well on fibronectin pre-coated 96-well plates under endothelial conditions. Endothelial medium was replaced twice per week. After 15 days in culture at 37°C and 5% CO_2, ECs colonies were counted, fixed with 4% paraformaldehyde (PFA, Electron Microscopy Sciences), and analyzed by immunofluorescence.

Characterization of hPSC-ECs

All the *in vitro* hPSC-EC characterization tests were carried out with confluent hPSC-ECs at passage 2. Replicates correspond to hPSC-ECs obtained from independently performed hPSC-differentiation experiments. Endothelial-colony forming cells (ECFC) isolated from human umbilical cord blood and cultured following the protocol described somewhere else (42) were used as positive control.

LDL uptake assay- hPSC-ECs and ECFCs were incubated with endothelial media supplied with 15 µg/mL of AF488-conjugated acetylated-LDL (Invitrogen) for 4 hours at 37°C and 5% CO_2. After incubation, endothelial media was removed. ECs were rinsed with PBS and fixed with 4% PFA in PBS for further immunofluorescence analyses.

Endothelial activation by TNF-α- hPSC-ECs and ECFCs were incubated with endothelial media supplied with 10 ng/mL of TNF-α (Miltenyi) overnight at 37°C and 5% CO_2. Next day, TNF-α-treated and non-treated

hPSC-ECs and ECFCs were analyzed for ICAM-1 expression by flow cytometry.

Nitric Oxyde (NO) detection- hPSC-ECs and ECFCs were incubated with endothelial media supplied with 0,5% FBS and 1µM DAF-FM-2A (Invitrogen) during 1h at 37°C and 5% CO_2. Positive controls were stimulated with 100 ng/mL LPS during the night preceding the experience. After incubation with the probe, cells were washed, and fluorescence was analyzed by flow cytometry.

Matrigel-based tube formation assay- hPSC-ECs and ECFCs were detached enzymatically from the culture plates with Accutase and seeded on a layer of 9 mg/mL Matrigel (Corning) at 20000 cells/cm^2 with endothelial media for 24h at 37°C and 5% CO_2. ECs were imaged every two hours with an inverted phase contrast microscope (Leica) and images were analyzed with the Image J tool Angiogenesis analyzer (Carpentier G. Contribution: angiogenesis analyzer. ImageJ News. 2012;5). Analyses herein shown correspond to quantification of 8h-images when the maximum number of networks was obtained. At 24h, cells were fixed and analyzed by immunofluorescence.

Transduction of hPSC-ECs

hPSC-ECs derived from SA01 cell line were transduced with a lentiviral vector carrying the red fluorescence protein mCherry under the control of a CMV promoter (LV-CMV-mCherry-Puro, SignaGen Laboratories). 24 hours after seeding hPSC-EB-$CD144^+$ under endothelial conditions, cells were incubated with the lentiviral vector at multiplicity of infection (MOI) 10 for 12 hours at 37°C and 5% CO_2 in the presence of 8 µg/mL polybrene (Sigma-Aldrich). After incubation, medium was replaced, and hPSC-ECs from SA01 cell line were recovered once they reached confluency. The transduction efficiency and the endothelial phenotype was evaluated by flow cytometry analysis. Only hPSC-ECs from SA01 cell line having more than 80% $mCherry^+$ cells were used for *in vivo* experiments.

Colony forming cell (CFC) assay

6 days-old hPSC-BCs were recovered and seeded for CFC assay at a density of $5x10^4$ cells/mL in MethoCult GF (H4435 StemCell Technologies) and Iscove's Modified Dulbecco's Medium (Gibco). Replicates correspond to hPSC-BCs obtained from independently performed hPSC-differentiation experiments. At day 14, hematopoietic CFCs (BFU-E, CFU-GM and CFU-GEMM) were counted and classified according to standard morphological criteria.

Immunofluorescence microscopy

As previously described in earlier sections, samples were fixed with 4% PFA in PBS for 10 minutes and washed with PBS. Samples were further permeabilized with PBS 0,1% Triton, blocked with PBS 5% bovine serum albumin (BSA, Eurobio) and incubated with primary antibodies diluted according to the manufacturer's conditions or previous experiences in PBS 1% BSA during 1h at 37°C. Excess of primary antibody was rinsed with PBS and samples were incubated with fluorochrome-conjugated secondary antibodies (supplementary table 1) and DAPI (Life technologies) for 1h at 37°C. After three washes with PBS, samples were mounted with Glycergel Mounting Medium (Dako). To verify the specificity of the

conjugated secondary antibodies, control samples were treated following the aforementioned conditions in absence of primary antibodies. Immunofluorescence images were acquired with the confocal microscope Leica TCS SP5 (Leica) and analyzed with software ImageJ.

Some adaptations of this protocol were necessary for treating hPSC-EB-CD144^{+} samples and the dorsal skinfold chambers. In both cases, incubation with 4% PFA was extended to 4 hours. For the dorsal skinfold chambers, the epidermis still present at one side of the chamber was manually removed from the dermis. Permeabilization and blocking time were extended to 2 hours at room temperature and incubation of primary and secondary antibodies was performed overnight.

Sorting and cell analysis by flow cytometry

Cell analysis- hPSC single-cell suspensions were incubated with fluorochrome-conjugated antibodies against the human pluripotency markers SSEA-3, SSEA-4 and TRA-1-81 (BD Sciences). Single-cell suspension of hPSC-EBs, hPSC-ECs, hPSC-BCs and ECFCs were incubated with fluorochrome-conjugated mouse antibodies recognizing the human hematoendothelial markers CD34 (BD Sciences), CD143 (Miltenyi), and CD309 (Miltenyi), the endothelial markers CD144 and CD31 (Miltenyi), and the hematopoietic markers CD43, CD45, and CD41a (BD Sciences) (supplementary table 1). For the intracytoplasmic detection of eNOS, hPSC-ECs and ECFCs were treated with the FIX & PERM Cell Permeabilization Kit (Thermofisher) according to the manufacturer's instructions and incubated with mouse PE-conjugated antibody against human eNOS. For, TNF-α activation tests, hPSC-ECs and ECFCs were incubated with anti-ICAM-FITC (Miltenyi). Blood samples from the NSG mice from the hematopoietic reconstitution experiences were treated with the ACK lysis buffer (Gibco) according to the manufacturer instructions to lyse red blood cells. Lysed blood samples and bone marrow mouse samples were further incubated with specific anti-human CD45 (BD Sciences). Cells were incubated with either the selected antibodies or the equivalent FITC-, PE- and APC-conjugated isotypes for 30 minutes on ice, washed and resuspended in PBS containing 5% FBS and 1µg/mL of 7AAD to exclude dead cells. Data acquisition was performed with the BD Accuri C6 cytometer and analyses were carried out with the BD Accuri C6 Plus Software (BD Biosciences).

Cell sorting- Single-cell suspensions were incubated with anti-SSEA3-AlexaFluor647 for isolation of SA01 hPSCs, anti-CD144-PE for isolation of 84h-hPSC-EB-CD144^{+}, and anti-CD144-PE and anti-CD45-FITC for isolation of hPCS-BC-CD144^{+}CD45^{+} following the same procedure as described in the section *cell analysis*. Selected populations were isolated with a BD FacsAria Sorter (BD Biosciences).

RT and qPCR

Total mRNA from hPSCs, 48h-hPSC-EBs, 84h-hPSC-EBs, hPSC-EB-CD144^{+}, hPSC-EB-CD144^{-}, hPSC-ECs, hPSC-BCs and red CFC (BFU-E + CFU-GEMM) was extracted with the RNeasy Micro Kit (Qiagen) and quantified with the NanoDrop™ 1000 Spectrophotometer (Thermo Fisher Scientific). Reverse transcription (RT) was further performed by using the SuperScript III kit (Invitrogen) with random hexamers. Three replicates per sample, each corresponding to 9 ng of cDNA, were analyzed for differential gene

expression by using the Mx3000P qPCR thermocycler system (Agilent) with Brilliant III Ultra-Fast SYBR Green (Agilent) for most of the genes and with TaqMan Universal Master Mix II, no UNG (Applied Biosystems) for arterial/vein endothelial genes as shown in supplementary tables 2 and 3. mRNA extraction and RTqPCR conditions were set according to the manufacturer's instructions. Target gene expression was normalized with the endogenous RNA control human 18S and ERCC3 according to the $2^{-\Delta\Delta Ct}$ method. Fold-change expression was calculated with respect to the initial hPSCs of the same differentiation experiment for *NANOG, POU5F1, TBXT* and *KDR. ETV2* and *RUNX1* fold-change expression in $CD144^{+}$-hPSC-EBs and $CD144^{-}$-hPSC-EBs was calculated with respect to non-sorted 84h-hPSC-EBs. For arterial/venous phenotype, expression is relative to ECFCs gene expression. Finally, for the hematopoietic genes, mRNA expression was compared to total human BM gene expression.

For the mouse BM samples from the hematopoietic reconstitution experiments, qPCR was also used to quantify the presence of human CD45 DNA. DNA was extracted according to the instructions of the GeneJET Genomic DNA Purification kit (ThermoFisher Scientific) and quantified with the NanoDrop™ 1000 Spectrophotometer. Three replicates per sample, each corresponding to 36 ng of DNA, were analyzed for the presence of human CD45 DNA and normalized based on the mouse actin gene (supplementary table 4).

In vivo **experiments**

Ischemic tissue injury model on a mouse dorsal skinfold chamber- 8-week-old male nude mice were obtained from the Animal Core Facility of Gustave Roussy Institute. The surgical procedure followed a previously described protocol (43). Briefly, after 100 µL subcutaneous injection of Lidocaine (21.33mg/mL), the dorsal skinfold of an anesthetized mouse (mix 1.5% isoflurane with air at 1.5 L/min) was stretched keeping the dorsal median line at the top. The two faces of the dorsal chamber were positioned on each side of the skinfold and secured by sutures between two adjacent orifices. To prepare the side of the chamber where cells would be injected, the entire epidermis and upper dermis were removed as close as possible to the edges of the chamber. 15 nude mice were grouped in 3 experimental groups as follows. 6 nude mice were injected intradermally on the dorsal chamber with $3x10^5$ mcherry hPSC-ECs from SA01 cell line resuspended in 20 µL of PBS. On 9 nude mice, an ischemia was induced by thermal cauterization of a macrovessel 15 minutes before cell injection; 6 of them were further injected with $3x10^5$ mcherry hPSC-ECs resuspended in 20 µL of PBS and 3 of them with 20 µL of PBS. In all the cases, hPSC-ECs or PBS controls were injected next to the cauterized blood vessel. The injected side of the chamber was covered with a glass coverslip sealed under mechanical pressure by the rings. A subcutaneous injection of Tolfédine (4mg/kg) was administrated at the end of the surgical procedure before mouse awakens. Mice were maintained for a maximum of 30 days after dorsal chamber implantation. Once per week, anesthetized mice (mix 1.5% isoflurane with air at 1.5 L/min) were injected with 70kDa-FITC dextran intravenously in the retro-orbital sinus (100 µL) and images of the dorsal chamber were acquired with a confocal microscope (SP8, Leica) in brightfield and fluorescence mode. At day 30, after the last acquisitions, mice were euthanatized by progressive doses of CO_2 according to

ethical guidelines, and the dorsal chambers were recovered to perform further immunofluorescence analyses as described above.

Quantification of the blood vessels at the dorsal skinfold chamber- Treatment of macroscopy images of the dorsal chambers was performed with the software ImageJ. PBS controls were used to set up the parameters for background subtraction and blood vessel quantification. The plugin Tubeness (44) followed by Analyze skeletons 2D/3D (45) were used on all the images following the parameters selected for the control. The density of blood vessels was reported as the total branch length measured in the dorsal chamber for day 5 and day 19 post-injection. For every mouse, we calculated the change in percentage of the total branch length of day 19 compared to day 5.

Hematopoietic reconstitution in irradiated immunosuppressed mouse- For the hematopoietic reconstitution, NOD.Cg-PrkdcscidIl2rgtm1Wjl/SzJ mice (NSG) obtained from the Animal Core Facility of Gustave Roussy Institute, were bred and maintained under specific pathogen free conditions with acidified water (pH 5.3). Six to eight-week-old mice were irradiated at 2.5 Gy with an IBL637 gamma irradiator containing a Cs-137 source. After 24 hours, mice were subjected to isoflurane anesthesia and submitted to intra-BM transplantation (IBMT) in the right femur with $4x10^5$ hPSC-EB-CD144$^+$ in 15 µL PBS. Peripheral blood was obtained from the retro-orbital sinus of anesthetized mice and analyzed at 6 weeks post-transplant for the presence of human hematopoietic cells by flow cytometry analysis as described previously (46). Mice were euthanatized at 12 weeks post-transplant. BM cells were collected and analyzed for the presence of human hematopoietic cells (hCD45) by flow cytometry. Genomic DNA was extracted from the BM of the right (injected) and left (non-injected) femurs and analyzed by quantitative PCR (Q-PCR) as described in materials.

Human EL isolation and cell preparation

Human embryos (range 7–8 weeks of gestation) were obtained following voluntary abortions. Developmental age was estimated based on several anatomic criteria according to the Carnegie classification for embryonic stages 74 and by ultrasonic measurements. ELs were excised sterilely using microsurgery instruments and a dissecting microscope in phosphate-buffered saline (PBS) supplemented with 10% fetal bovine serum (FBS, Hyclone Laboratories). ELs were then disrupted mechanically through successively 18-, 23- and 26-gauge needles. Cells clumps were removed on a 70 µm nylon filter (Invitrogen), washed three times with Dulbecco's modified eagle medium (DMEM; Gibco)/FBS 10% and quantified. Mononuclear cells were isolated using Pancoll centrifugation gradient (Dominique Dutscher). Mononuclear cells from human EL were incubated with anti-CD45-FITC, anti-CD144-PE and anti-CD34-APC antibodies for 30 min at 4°C. Selected CD144$^+$CD45$^-$CD34$^+$ EL-EC, CD144$^+$CD45^{low}CD34$^+$ EL-pre-HSC, CD144$^-$CD45^{low}CD34$^+$ EL-HSC/HP and CD144$^-$CD45^{high}CD34$^-$ mature EL-HC cell populations were sorted by flow cytometry (Table 2) as described previously (Oberlin et al., 2019).

Table 2
Human embryonic liver (EL) sorted cell populations.

Sorted cell population	Name
EL $CD144^{+}CD45^{-}CD34^{+}$cells	EL-ECs
EL $CD144^{+}CD45^{low}CD34^{+}$cells	EL-pre-HSCs
EL $CD144^{-}CD45^{low}CD34^{+}$cells	EL-HSCs/HPs
EL $CD144^{-}CD45^{high}CD34^{-}$cells	EL-mature HCs

Transcriptomic analyses

For the transcriptomic study hPSC-ECs, hPSC-EB-$CD144^{+}$, hPSC-BCs and hPSC-BC-$CD144^{+}CD45^{+}$ (Table 1) were derived from undifferentiated hESC (H1 cell line). $CD144^{+}CD45^{-}CD34^{+}$ EL-EC, $CD144^{+}CD45^{low}CD34^{+}$ EL-pre-HSC, $CD144^{-}CD45^{low}CD34^{+}$ EL-HSC/HP and $CD144^{-}CD45^{high}CD34^{-}$ EL-mature HC cell populations were freshly isolated from human EL (Table 2). RNAs were purified using Direct-Zol ™RNA kit (ZymoResearch) according to manufacturer's protocol. After validation of the RNA quantity and quality with the Bioanalyzer 2100 (using Agilent RNA6000 nano chip kit), 10 ng of total RNA was reverse transcribed following the Ovation PicoSL V2 system (Tecan). Briefly, the resulting double strand cDNA was used for amplification based on SPIA technology. After purification according to Tecan protocol, 3.6 ug of Sens Target DNA were fragmented and biotin labelled using Encore Biotin Module kit (Tecan). After control of fragmentation using Bioanalyzer 2100, cDNA was then hybridized to GeneChip® HumanGene 2.0 ST (Affymetrix) at 45°C for 17 hours. Chips were washed on the fluidic station FS450 following specific protocols (Affymetrix) and scanned using the GCS3000 7G. The scanned images were then analyzed with Expression Console software (Affymetrix) to obtain raw data (cel files) and metrics for Quality Controls. RMA normalization was performed using TAC4.0 software (Thermofisher) with default parameter.

Data were first explored with unsupervised learning methods using the Perseus software platform (http://www.perseus-framework.org) v1.6.14.0 to perform principal component analyses and hierarchical clustering (with Pearson correlation).

Supervised analyses were performed using TAC4.0 software to identify transcripts specifically up- or down-regulated in each pairwise cell population comparison (supplementary Fig. 4). For each cell population, a Tukey's Biweight Robust Mean is calculated from log2 expression values. Mean ratio is then calculated from unlog mean values. If ratio > 1 then FoldChange = ratio, and if ratio < 1 then FoldChange = -1/ratio. Statistical pValue is calculated after ANOVA test using ebayes model.

Enrichments were also explored using GSEA (Gene Set Enrichment Analysis) v4.1.0 software (https://www.gsea-msigdb.org/gsea/). Gene Set Enrichment Analysis determined whether gene sets from the Molecular Signatures Database (MSigDB) Gene Ontology Biological Process collection

(c5.go.bp.v7.4) were randomly distributed throughout our ranked transcript lists or if they were located at the top or bottom of them. The selected parameters were: Signal2Noise metric, gene set permutation (n = 1000).

Datasets generated and analyzed during the current transcriptomic study are available in GEO (accession number GSE194372) and can be queried via the following link [https://www.ncbi.nlm.nih.gov/geo/query/acc.cgi?acc=GSE194372].

Statistics analyses

Sample sizes were determined by the nature of the experiment and variability of the output, not by a statistical method. Statistical analyses were performed in PRISM software. Data obtained from multiple experiments were reported as mean ± standard error. n = 5 in most all the experiments unless stated differently. Where appropriate, either a paired parametric t-test or a one-way ANOVA with a Tukey post-hoc test. Differences were considered significant when *$p < 0.05$, **$p < 0.005$, or ***$p < 0.0005$.

Results

hPSCs differentiation into CD144^{+}hematoendothelial progenitors

hPSC-EBs were generated from one hiPSC line, A29, and two hESC lines, SA01 and H1, following an adapted version of the Lu et al. protocol (47). Briefly, mesoderm was induced during the first 48 hours of hPSC-EB formation followed by hematoendothelial specification step from the mesoderm during the next 36 hours in a serum-free medium (Fig. 1A). A progressively loss of pluripotency during hPSC-EB formation was confirmed by a decreased in the mRNA levels of two pluripotency markers, *POU5F1 (OCT3/4*) and *NANOG*, for all hPSCs (Fig. 1B-C). This loss of pluripotency coincided in time with a peak in the expression of the mesodermal marker *TBXT* at 48h (Fig. 1D) followed by a significant increase in the expression of *KDR* (CD309) at 84h of hPSC-EB formation (Fig. 1E). No significant differences in this kinetics were observed among the hPSC lines.

Since *KDR* (CD309) has been described as an important marker of endothelial and hematopoietic precursors (48), we hypothesized that the increased in *KDR* expression may mark the apparition of hematoendothelial progenitors within 84h-hPSC-EBs. Thus, we analyzed the expression of other endothelial and hematopoietic markers in 84h-hPSC-EB by flow cytometry (Fig. 1F). Between 15–25% of cells within 84h-hPSC-EBs expressed hematoendothelial markers as CD309, CD34 and CD143, and the endothelial marker CD144, independently on the hPSC line. Fewer cells (≈ 10%) expressed the endothelial marker CD31 and almost none expressed the hematopoietic markers CD43, CD45 and CD41. Interestingly, the CD309^{+} population did not contain exclusively hematoendothelial progenitors since only 60% of these CD309^{+} cells coexpressed CD34, CD143 and CD144 (supplementary Fig. 1). Instead, the CD144^{+} population seemed a more homogeneous population composed by more than 90% of

$CD34^+CD143^+CD309^+$ cells (Fig. 1G). CD144 is a classical endothelial marker expressed by both hemogenic and non-hemogenic endothelium. Thus, the $CD144^+$ population was isolated from 84h-hPSC-EBs as a possible source of both ECs and HCs cells. As expected, hPSC-EB-$CD144^+$ expressed significantly higher levels of two master transcription factors required for endothelial and hematopoietic specification, *ETV2* and *RUNX1*, compared to the non-sorted 84h-hPSC-EBs and hPSC-EB-$CD144^-$ (Fig. 1H-I). No significant differences among the hPSC lines were observed. These results suggest that hPSC-EB-$CD144^+$ may contain not only ECs but also hemogenic ECs.

hPSC-EB-$CD144^+$ generates functional and mature hPSC-ECs

We, then, first sought to determine whether hPSC-EB-$CD144^+$ include proliferative endothelial progenitors. hPSC-EB-$CD144^+$ were seeded at one cell per well in a 96 well plate. Small colonies were observed at day 7 and kept growing until day 15 confirming the existence of proliferative ECs within hPSC-EB-$CD144^+$ (Fig. 2A-B). Similar results were obtained when fresh and frozen hPSC-EB-$CD144^+$ were cultured at a normal cell density. hPSC-EB-$CD144^+$ differentiate into cobblestone-like cells that proliferate until reaching confluence (Fig. 2C). hPSC-ECs were composed of more than 90% cells expressing CD144, CD31, CD34 and vWF (Fig. 2D-E). Most of these cells also expressed CD309 and CD143. We did not observe expression of the hematopoietic markers CD43, CD45 and CD41 (Fig. 2D). hPSC-ECs could be maintained in culture up to 6 passages without modifying their endothelial phenotype (Fig. 2C-D). However, the cumulative population doublings (CPD) decreased during time suggesting hPSC-ECs do not proliferate indefinitely (Fig. 2F). It is worth to note that the CPD was dependent on the hPSC line, being generally smaller for hPSC-ECs coming from A29 compared to hPSC-ECs derived from SA01 and H1.

Next, hPSC-EB-$CD144^+$ were cultured in the presence or absence of an inhibitor of Notch pathway (DAPT). Notch signaling pathway plays a pivotal role in arterial but not in venous differentiation (49). hPSC-EB-$CD144^+$ proliferated and formed a confluent homogeneous layer of hPSC-ECs in both conditions, independently on the hPSC line of origin (supplementary Fig. 2). Their endothelial identity was confirmed by flow cytometry analysis showing that more than 95% of cells expressed CD309, CD144, CD31, CD34 and CD143 independently on the presence or absence of DAPT. No expression of the hematopoietic markers CD43 was detected (supplementary Fig. 2). Similarly, RTqPCR analysis revealed no differences in the expression of the panendothelial marker *CDH5*, suggesting than inhibition of the Notch pathway does not affect the differentiation of hPSC-EB-$CD144^+$ into hPSC-ECs. No differences in the expression of the arterial marker *NRP-1* were observed between DAPT-treated and untreated ECs (Fig. 2G-I). However, DAPT-treated ECs downregulated the arterial marker *EFNB2*. Some heterogeneity between hPSC lines was observed regarding the expression of venous markers. While hPSC-EC from A29 cell line cultured in the presence of DAPT showed a significantly higher expression of *NRP2, EPHB4* and *NR2F2* compared to the control, hPSC-EC from SA01 and H1 cell lines only showed upregulation of *NRP2* and *NR2F2*, and *NR2F2*, respectively (Fig. 2G-I). These results suggest that the hPSC-EB-$CD144^+$ arterial/venous specification may

be guided *in vitro* under the appropriate culture conditions although their response to environmental factors might be influenced by the hPSC line from which they are derived.

We also investigated whether hPSC-EB-CD144^{+} were able to differentiate into fully mature ECs *in vitro.* To this, we compared the *in vitro* functionality of hPSC-ECs to human umbilical cord blood endothelial progenitors, ECFCs. Ac-LDL was observed in the cytoplasm of hPSC-ECs derived from A29, SA01 and H1 hPSCs like ECFCs (Fig. 3A) after 4h of incubation with a fluorochrome-conjugated ac-LDL, suggesting hPSC-ECs are able to endocyte LDL. In addition, more than 90% of hPSC-ECs and ECFC expressed high levels of the adhesion molecule ICAM-1 in response to TNF-α. In contrast, less than 1% of untreated cells expressed similar levels of ICAM-1 suggesting hPSC-ECs may be activated by proinflammatory cytokines (Fig. 3B).

All hPSC-ECs formed a tubular network comparable to the one formed by ECFCs after seeding on Matrigel (Fig. 3C, 3C' and supplementary Fig. 2). No significant differences in the number of master segments and meshes, neither in the total segment length nor in the branching length were observed among hPSC lines and ECFCs. However, ECFCs formed networks with a slightly reduced number of segments, nodes and branching intervals compared to hPSC-ECs (Fig. 3C').

Production of nitric oxide (NO) by the endothelial nitric oxide synthase (eNOS) is known to play an important role in endothelial homeostasis, inflammation, and vasodilation. We detected eNOS in 72 to 86% of hPSC-ECs and 84.5% of ECFCs (Fig. 3D). We further analyzed NO production by using the probe DAF-FM diacetate. This permeable molecule is de-acetylated inside the cell and reacts with NO to form fluorescent DAF-FM that can be detectable by flow cytometry. In the absence of the probe, no fluorescence was detected for any of the hPSC-ECs nor ECFCs. However, after incubation with the probe, we detected the fluorescent DAF-FM in 83 to 92% of hPSC-ECs and 88% of ECFCs (Fig. 3D'). Slightly increase of DAF-FM fluorescence was detected when ECs were incubated with LPS (known to induce the NO production) and with a S-nitrosothiol molecule (SNAP) as a positive control.

Finally, we tested the *in vivo* angiogenic potential of hPSC-ECs in a mouse dorsal chamber model where an ischemic injury has been induced. Since not apparent differences in the functionality of the three hPSC-ECs were observed *in vitro*, we performed the *in vivo* experiments with mcherry-ECs derived from SA01 cell line. mcherry-ECs were detected for 4 weeks in the mice. Real time *in vivo* imaging showed that mcherry-ECs migrated and localized around the proximities of mouse blood vessels at day 5 independently on the induction or not of an ischemia. Intravital microscopy analysis demonstrated hPSC-ECs appear to line up around blood vessels and capillaries (Fig. 3E). Quantification of the blood vessels show no significant differences between the analyzed conditions, although the number of new blood vessels was slightly higher in mice injected with mcherry-ECs (Fig. 3F, supplementary Fig. 3). The immunofluorescent analysis post-mortem confirmed the survival of human CD144^{+} hPSC-ECs in both ischemic and non-ischemic mice and their localization at the wall of the blood vessels. No teratomas or any other complications were observed at the dorsal chambers. Thus, SA01-ECs survive and participate to the formation of new vessels *in vivo* (Fig. 3G).

hPSC-EB-CD144^{+} contain hemogenic hPSC-ECs

To confirm the existence of hemogenic ECs within the hPSC-EB-CD144^{+} population, fresh and frozen hPSC-EB-CD144^{+} and hPSC-EB-CD144^{-} cells were seeded on a serum-free methylcellulose enriched with hematopoietic cytokines. After 4 to 6 days, hPSC-BCs were observed for the three-hPSC lines only in the CD144^{+} fraction (Fig. 4A). Flow cytometry analysis showed that more than 90% of hPSC-BCs were positive for the hematopoietic marker CD43 (Fig. 4B). Analyses of other hematopoietic and endothelial markers revealed heterogeneity within hPSC-BCs. Between 33 to 62% of hPSC-BCs expressed CD41 and 33 to 56% of hPSC-BCs expressed CD45 (Fig. 4B). In addition, a subpopulation of hPSC-BCs coexpressed the hematoendothelial markers CD34 and CD143 (11–46%). Interestingly, only a small fraction of hPSC-BCs retained the expression of CD144 and around 5 to 25% of hPSC-BCs co-expressed CD144 and CD45 markers (Fig. 4C) suggesting that hPSC-EB-CD144^{+} may undergo endothelial-to-hematopoietic transition (EHT) to give rise to HCs. Even though hPSC-BCs were observed from all the three-hPSC lines, significant differences in the expression of hematopoietic and endothelial markers were observed among the hPSC-BCs. Notably, hPSC-BCs from H1 expressed significantly more CD34, CD143, CD45 and CD41, suggesting a difference in hematopoietic potential among the hPSC cell lines (Fig. 4B-C).

We further analyzed the expression of key hematopoietic transcription factors in hPSC-BCs compared to hPSC-EB-CD144^{+} and hPSC-ECs RTqPCR. Consistently with their common origin and the role of *SCL* and *GATA2* in both endothelial and hematopoietic differentiation, *SCL* and *GATA2* mRNAs were detected in hPSC-EB-CD144^{+}, hPSC-ECs and hPSC-BCs independently on the hPSC-line (Fig. 4D-E). However, the expression of *SCL* was significantly higher in hPSC-BCs for A29 and SA01 (Fig. 4D). hPSC-BCs expressed significantly higher levels of the *RUNX1* isoform c and *GATA1*, transcription factors implicated in HSC emergence and erythropoiesis, respectively (Fig. 4F-G). In addition, hPSC-BCs expressed reduced levels of *HOXA3* compared to hPSC-EB-CD144^{+} and hPSC-ECs, a transcription factor key for arterial and hemogenic endothelium determination (Fig. 4H).

Given the hematopoietic profile of hPSC-BCs, we next assessed hPSC-BC hematopoietic potential *in vitro*. hPSC-BC derived from hiPSCs and hESCs lines gave rise to myeloid and erythroid colonies CFU-GM, CFU-GEMM and BFU-E with an efficiency of 79 to 117 CFU per 10^5 seeded hPSC-BCs (Fig. 5A-B). From these, most of the colonies accounted for CFU-GM (60% – 87%), around 22–38% corresponded to BFU-E and only 0.1–4% were CFU-GEMM, confirming the heterogeneity previously described by flow cytometry (Fig. 5C). Although similar percentages were found for the three hPSC lines, it is worth to note that hPSC-BCs from SA01 generated slightly more CFU-GEMM (4.3 ± 2.4%) than A29 cell line (0.1 ± 0.4%) and H1 (0.8 ± 0.9%) (Fig. 5C). Since hemoglobin subunits are differentially expressed during the embryonic, fetal, and adult erythropoiesis, we analyzed by RTqPCR the expression of the embryonic (ε), fetal (γ) and adult (β) hemoglobin chains from hPSC-derived CFU-GEMM and BFU-E colonies and we compared them to the embryonic human liver transcripts. CFU-GEMM and BFU-E derived from hPSCs expressed significantly higher levels of ε hemoglobin (*HBE1*) ($10–10^3$ -fold change) compared to ELs (Fig. 5D). In contrast, all the hPSC-derived hematopoietic colonies expressed significantly less γ (*HBG1*) (0.025-0.12-fold change)

and β (HBB) hemoglobin ($7x10^{-5}$-$1x10^{-4}$-fold change) than human ELs (Fig. 5D). In other words, hPSC-derived CFU-GEMM and BFU-E expressed around 10^2 times more ε than β hemoglobin (Fig. 5E). These results suggests that our protocol yields principally embryonic erythrocytes and to lesser extent, definitive erythrocytes.

To confirm the existence of bona fide HSCs/HPs in hPSC-EB-CD144$^+$, we analyzed the *in vivo* hematopoietic reconstitution potential of hPSC-EB-CD144$^+$ in a xenograft model of immunodeficient NSG mice. When hPSC-EB-CD144$^+$ from H1 were intravenously injected, we did not observe any hematopoietic engraftment in the transplanted mice while human cord blood CD34$^+$ cells engrafted efficiently (data not shown). To circumvent any caveat due to homing defects, we injected hPSC-EB-CD144$^+$ cells directly into the right femur of sublethally irradiated NSG mice by intra-BM transplantation (IBMT). Mice were monitored for human reconstitution by peripheral blood analyses (at 6 weeks, see Table 3) and were euthanatized at 12 weeks post-transplant. BM was, then, analyzed for human CD45 expression by FACS analysis and the presence of human DNA in the BM of the right and left femur of transplanted mice was also analyzed by qPCR. Six weeks after transplantation, we observed human CD45$^+$ cells in the peripheral blood of mice injected with CD34$^+$ cells (1% and 9%) and with hPSC-EB-CD144$^+$ from H1 (between 0.5% and 3.6%). We did not detect any human CD45$^+$ in the control mice injected with PBS (Table 3). After 3 months of engraftment, human specific CD45 was detected by flow cytometry only in the right femur in 5 out of 5 mice injected with hPSC-EB-CD144$^+$ from H1 (between 0,1% and 0,6%) (Table 3). In the mice injected with human umbilical cord blood CD34$^+$ cells as control, human specific CD45 was detected in both right (9% and 10%) and left femurs (1% and 5%) (Table 3). These results were further confirmed by qPCR where CD45 human specific DNA was detected in the right femur for hPSC-EB-CD144$^+$ and in the right and left femur for hCD34$^+$ cells from human cord blood. One left femur out of five was also positive for human DNA, however it was negative for CD45 in the flow cytometry analysis. Mice injected with PBS did not express human specific CD45 neither contained human DNA in the femurs (Fig. 5F). No developed lymph nodes or tumors were observed in any of the examined mice. These results suggest hPSC-EB-CD144$^+$ have a hematopoietic reconstitution potential only by IBMT however, this is considerably lower compared to human CD34$^+$ isolated from umbilical cord blood.

Table 3
Hematopoietic reconstitution in NSG mice.

Sample		Human CD34		hPSC-EB-CD144$^+$					PBS	
		#1	#2	#1	#2	#3	#4	#5	#1	#2
%hCD45 in the PB		9%	1%	1.5%	0.6%	0.5%	0.9%	3.6%	0%	0%
%hCD45	*RF*	10%	9%	0.1%	0.3%	0.1%	0.1%	0.6%	0%	0%
in the BM	*LF*	5%	1%	0%	0%	0%	0%	0%	0%	0%
Human DNA	*RF*	1	0.662	0.007	0.210	0.013	0.0004	0.051	ND	ND
Fold change	*LF*	0.175	0.008	ND	ND	0.0002	ND	ND	ND	ND

Percentage of human CD45$^+$ cells detected by flow cytometry in peripheral blood (PB) and in the bone marrow (BM) from right (RF) and left femur (LF) of NSG mice injected with either human CD34$^+$ cord blood cells, hPSC-EB-CD144$^+$ cells or PBS. Relative quantification of human DNA (based on the amplification of human CD45 gene) in BM of mice injected with human cells or PBS. ND: non detected.

Transcriptomic profile of CD144$^+$-EBs, hPSC-ECs and hPSC-BCs

To investigate whether hPSC-EB-CD144$^+$, hPSC-ECs and hPSC-BCs may correspond to their physiological equivalent, we performed a transcriptome analysis to compare hPSC-derived cell populations to undifferentiated hPSC, to differentiated-hPSC themselves and to human EL cell populations. In human, EL is considered as a major organ of hematopoiesis during development. From day 30 to the 30th week of human gestation, mature ECs (CD144$^+$CD34$^+$CD45$^-$) coexist with diverse hematopoietic populations resulted from the migration, proliferation, and maturation of HCs, namely pre-HSCs (CD144$^+$CD34$^+$CD45^{Low}), HSCs and HPs (CD144$^-$CD34$^+$CD45^{Low}) and mature HCs (CD144$^-$CD45^{High}) (14). Thus, EL allow us to compare hPSCs-derived cells to ECs and HCs, including intermediate pre-HSCs no longer found in adults but also HSCs/HPs and mature HCs, all with an identical genetic background.

We first confirmed the identity of the samples by a principal component analysis (PCA). As expected, undifferentiated-hPSCs and hPSC-derived populations were grouped in two independent groups (Fig. 6A). In addition, hPSC-derived cells did not cluster with EL samples, yet they were spatially closer to EL than to hPSCs (Fig. 6A). Independent PCA within each group (EL and hPSC-derived populations) clustered samples according to their endothelial and hematopoietic identity. As shown in Fig. 6B, EL sample distribution along the first component of EL-PCA showed a clear difference between EL-ECs and EL-mature HCs, located at the opposite extremes of the axis, while EL-pre-HSCs and EL-HSCs/HPs are in between these two populations, as result of the EHT giving place to HCs. A similar analysis within hPSC-derived cells clustered hPSC-EB-CD144$^+$ and hPSC-ECs in a separate group from hPSC-BC-CD144$^+$CD45$^+$ sorted and unsorted hPSC-BCs (Fig. 6C). Supervised analysis performed to identify transcripts

specifically up- or down-regulated in hPSC-derived cell populations confirmed these results. Indeed, when hPSC-ECs and hPSC-BC-CD144^{+}CD45^{+} were compared to hPSC-EBs, EC gene signatures were identified specifically in hPSC-ECs, whereas hemogenic and hematopoietic cell gene signatures were found in hPSC-BC-CD144^{+}CD45^{+}, confirming distinct endothelial, hemogenic endothelial and hematopoietic transcriptional profile in hPSC-derived populations (Fig. 6D).

To confirm these results, we performed a Gene Set Enrichment Analysis (GSEA) between each hPSC-derived cell population and undifferentiated hPSCs. hPSC-EB-CD144^{+} expressed a discrete list of endothelial and hematopoietic-related terms (see Fig. 6E and supplementary table 5), including *Embryonic Hemopoiesis* and *Endothelium Development* ones. Endothelial terms were mainly enriched in hPSC-ECs and hPSC-EB-CD144^{+} compared to hPSC-BC-CD144^{+}45^{+} and hPSC-BCs (Fig. 6E-G and supplementary table 5). In addition, hematopoietic terms including *Embryonic_Hemopoiesis* were enriched in hPSC-EB-CD144^{+}, hPSC-BCs and hPSC-BC-CD144^{+}45^{+} but not in hPSC-ECs (Fig. 6E-G and supplementary table 5). From all the hPSCs-derived populations, hPSC-ECs contained the larger group of endothelial-related terms, including the following *Blood vessel morphogenesis*, *Endothelial Proliferation*, *Lymphangiogenesis and Endothelial Barrier* (see Fig. 6F and supplementary table 5). hPSC-ECs display also few terms involved in HSCs/HPs differentiation and term related to erythroid, myeloid, and megakaryocytic hematopoietic lineages. In contrast to hPSC-EC, hPSC-BCs and hPSC-BC-CD144^{+}CD45^{+} contained a larger list of hematopoietic-related terms involved principally in the differentiation of HSCs/HPs and the maturation of HCS from erythroid, myeloid, megakaryocytes but also terms related to lymphoid lineages (see Fig. 6G and supplementary table 5). It is worth to mention that the terms related to leukocytes, lymphocytes and immune system were largely more enriched in hPSC-BC-CD144^{+}CD45^{+} than in unsorted hPSC-BC (Fig. 6G). These results suggest that hPSC-BC and more specifically hPSC-BC-CD144^{+}CD45^{+} have the potential to generate multilineage hematopoiesis contrary to hPSC-EB-CD144^{+} that were only enriched in terms involved in erythroid, myeloid, and megakaryocytic lineages (see supplementary table 5).

Once confirmed the identity of hPSC-derived populations, we performed an unsupervised hierarchical clustering between the hPSC-derived populations and the EL populations. As illustrated in Fig. 6H, two main clusters were obtained coinciding with the origin of the samples and not with their identity (*e.g.* endothelial or hematopoietic). An exception was observed for EL-HSCs/HPs, which were clustered together with non-sorted hPSC-BCs and hPSC-BC-CD144^{+}CD45^{+}, suggesting these two hPSC-derived populations are closed to physiological EL-HSCs/HPs (Fig. 6H).

We then performed a GSEA between hPSC-derived populations and their closest EL-equivalent population. Compared to EL-pre-HSCs, hPSC-EB-CD144^{+} displayed a stronger endothelial signature. However, they were also enriched in a discrete list of terms related to EL-HSCs/HPs differentiation. This hematopoietic potential was further confirmed by GSEA between hPSC-EB-CD144^{+} and EL-ECs. Interestingly, we did not observe enriched terms related to mature hematopoietic lineages (supplementary table 6).

When hPSC-ECs were compared to EL-ECs, hPSC-ECs exhibited a more mature endothelial phenotype compared to EL-ECs since they were enriched on terms associated to endothelial function so as *platelet aggregation* or *myeloid-leukocyte migration* but also on terms related to HSCs/HPs differentiation (supplementary table 6).

Despite comparison between hPSC-derived populations and undifferentiated hPSC showed that hPSC-BCs have a hematopoietic signature, GSEA between hPSC-BCs and EL-HSCs/HPs revealed that hPSC-BCs were enriched in endothelial terms when compared to human EL-HSCs/HPs hematopoietic populations. Furthermore, hPSC-BCs were not enriched in hematopoietic multilineage-related terms when compared to EL-HSCs/HPs. In contrast, hPSC-BC-CD144^{+}-CD45^{+} exhibit a long list of terms related to multilineage hematopoietic progenitors when compared to EL-HSCs/HPs. Regarding their endothelial phenotype, hPSC-BC-CD144^{+}-CD45^{+} expressed more endothelial-related terms than EL-HSCs/HPs but surprisingly less than EL-pre-HSC (supplementary table 6). These results suggest hPSC-BC-CD144^{+}-CD45^{+} are more engaged towards hematopoietic lineages and have a largest multilineage potential compared to hPSC-BC and may correspond to a population in between EL-pre-HSCs and EL-HSCs/HSCs.

Thus, these transcriptomic analyses suggest that hPSC differentiation into endothelial and hematopoietic cells recapitulates the human hematopoietic developmental processes through an EHT leading first to primitive hematopoiesis progenitors and thereafter to definitive hematopoietic progenitors (Fig. 6I).

Discussion

In the last decades, an increasing need to generate *in vitro* multicellular entities that recapitulate better organ physiology has pointed out the importance of ECs and HCs in these models. These two populations develop in close relationship during human embryonic development and maintain a tight connection during adulthood. Despite this, hPSC protocols focuses on the differentiation into these lineages independently. Although, most of the differentiation protocols of hPSCs into HCs generate an intermediate hemogenic endothelium, they do not generate mature ECs *in vitro*. Here we modified a previously published protocol of hematopoietic hPSCs differentiation (47) by adding a WNT agonist, CHIR, during the first 48h of differentiation. Early activation of the WNT canonical pathway has been proven to support definitive hematopoiesis (50). After only 3 days of hPSC differentiation, we generated around 20% of a population of hematoendothelial cells. Similar percentages have been obtained previously with other protocols of endothelial and hematopoietic hPSC differentiation (51–54). We showed that CD144 is a more suitable marker than CD309 to isolate a population of endothelial progenitor-like cells capable of generating both hematopoietic and endothelial cells, characterized for the expression of other hematoendothelial markers such as CD34, CD143 and CD309 (47, 55, 56) and hematoendothelial transcription factors such as *ETV2, RUNX1, GATA2, SCL* and *HOXA3*. In fact, hPSC-EB-CD144^{+} can be frozen and/or differentiated further into mature ECs or HCs. Mature hPSC-ECs derived from these hematoendothelial progenitors were able to take up LDL, activated upon pro-inflammatory signals and synthesized NO *in vitro*. We demonstrated that EC differentiation can be guided *in vitro* to arterial or venous lineages. *In vivo*, they incorporated to host blood vessels as we showed in a murine

model of ischemia on a dorsal skinfold chamber. These results are similar to those previously obtained by our team using umbilical cord ECFCs (57). hPSC-ECs seem also to facilitate new blood vessel formation 1-month post-injection, as evidenced by a slightly increase in the number of blood vessels compared the control mouse injected with PBS. Ischemia did not seem to be necessary for the incorporation of new blood vessels since we observed human $CD144^+$ cells in both conditions. This may be caused by natural turnover of the host endothelial layer and replacement by hPSC-ECs or by the wound healing process following the surgical procedure leading to the formation of new blood vessels.

We showed hPSC-EB-$CD144^+$ contained also a hemogenic endothelium able to differentiate into hPSC-BCs and through these, generate erythroid and myeloid colonies. hPSC-BCs display a hematopoietic phenotype expressing CD43 and contained subpopulations expressing CD45, CD41, CD34 and/or CD143 which may correspond to different HPs populations. As observed in the CFC assay, only a minority (< 1%) of colonies corresponded to GEMM, suggesting the existence of very few multipotent HPs in hPSC-BCs. These CFU-GEMM and BFU-E expressed high levels of ε-globulins as expected from primitive HPs. However, adult β-globin transcripts in these colonies besides the expression of genes involved in definitive hematopoiesis such as *RUNX1* (and the isoform c), *GATA2* and *HOXA3* suggest that hPSC-EB-$CD144^+$ may also be able to generate definitive hematopoietic progenitors (18, 51, 54). Other studies generating definitive HPs from hPSCs require longer time of differentiation (26, 54) or coculture with stromal cells (58, 59). Since differentiation of hPSC-EB-$CD144^+$ into hPSC-BCs may not favor the maintenance of multipotent HPs, we injected hPSC-EB-$CD144^+$ and not hPSC-BCs in irradiated NSG mouse. We did not detect any human cells in mice that were injected intravenously. Instead, we were able to detect very few human $CD45^+$ cells in the BM of mice injected hPSC-EB-$CD144^+$ by IBM injections. These results confirm that hPSC-EB-$CD144^+$ may generate definitive progenitors under the right conditions but highlight the impossibility of these cells to migrate towards the hematopoietic niche. This is not a rare event since it has been previously documented that human hemogenic endothelium requires *in vitro* coculture with stromal cells in order to reconstitute hematopoiesis in host irradiated mouse (11).

Despite all hPSCs lines differentiate into endothelial and hematopoietic differentiation, we observed differences among them in terms of proliferation and response to DAPT in the case of hPSC-ECs, or expression of hematopoietic markers and CFC composition, in the case of hPSC-BCs. Many studies have reported differences among hPSCs lines, hESCs and hiPSCs (61–63). Our protocol is robust enough to generate both lineages in an efficient way from different hPSCs but allows variability among individuals which might be useful in fields such as developmental biology.

Transcriptomic analyses between hPSC-derived populations and undifferentiated hPSCs, between hPSC-derived populations themselves and against human EL-populations confirmed our results. hPSC-EB-$CD144^+$ display an hematoendothelial signature and were more enriched in endothelial terms than EL-pre-HSCs, as expected from a hemogenic endothelium. hPSC-ECs derived from hPSC-EB-$CD144^+$ did show characteristics of mature EL-ECs. Interestingly, hPSC-ECs expressed genes involved in lymphangiogenesis, suggesting hPSC-ECs may either contain progenitors of lymphatic ECs or retain

certain plasticity allowing them to differentiate further in lymphatic ECs. In addition, GSEA showed hPSC-ECs expressed genes related to HPs and hematopoiesis. Further analyses are required to determine whether this transcriptomic signature is a remnant of the hematoendothelial progenitor which they are differentiated from (hPSC-EB-CD144^{+}) or evidence of their supportive role in hematopoietic differentiation as in the hematopoietic niche (17, 58).

Regarding hPSC-BCs, comparison between hPSCs-derived populations showed that hPSC-BCs displayed a hematopoietic signature as it has been demonstrated in our study and by other authors (64, 65). hPSC-BCs were enriched in genes participating in embryonic hematopoiesis restricted to megakaryocytic, myeloid and erythroid lineages. Remarkably, hPSC-BCs were similarly enriched in endothelial-related terms compared to EL-pre-HSCs. At the end of the 20th century and beginning of the 21st century, several studies pointed out the bipotency of hPSC-BCs (47, 55, 64, 65), able to generate both endothelial and hematopoietic lineages. In 2009, Lancrin et al. demonstrated in mice that hPSC-BCs generate HCs through an endothelial intermediate (64). Our study demonstrated that hPSC-BCs are a heterogeneous population which contain a small fraction of CD144^{+}CD45^{+} cells. Rather than an intermediate of the differentiation of hPSC-EB-CD144^{+} into hPSC-BCs (hPSC-EB-CD144^{+} > hPSC-BC-CD144^{+}CD45^{+} > hPSC-BC-CD144^{-}CD45^{+}), our transcriptomic analyses suggest that hPSC-BC-CD144^{+}CD45^{+} are more engaged in hematopoiesis and contain more multilineage progenitors involved in the differentiation of definitive HCs such as lymphoid cells than hPSC-BCs and that they may correspond to a population in between EL-pre-HSCs and EL-HSCs/HSCs. Thus, our hematopoietic differentiation protocol of hPSC-EB-CD144^{+} seems to recapitulate *in vitro* both primitive and definitive hematopoiesis. Isolation and expansion of these hPSC-BC-CD144^{+}CD45^{+} subpopulation should be explored in the future as a potential source of human HSCs.

Conclusion

In conclusion, herein we presented a differentiation protocol of hematopoietic and endothelial cells through a hematoendothelial population. This intermediate population is obtained after 84 hours of hPSC-EB formation following CD144-based cell sorting. These cells can be frozen without altering their bipotential properties. Their endothelial and hematopoietic progeny are considered as pure because they are not mixed populations of both lineages. This protocol was shown to be reproducible; hPSC-ECs and hPSC-BC-CD144^{+}CD45^{+} were obtained independently on the hESC and hiPSC used. Comparison hPSC derived cells with human EL subpopulations showed similarities between these hPSC derived cells and their physiological human EL counterpart and help to define a developmental hierarchy between hPSC derived cells themselves. Finally, hPSC-ECs and hPSC-BC-CD144 + CD45 + subpopulation were proven to be good candidates for future cell therapy. Therefore, hPSC-EB-CD144^{+} are an interesting and rapid source of ECs and HCs for tissue engineering.

Declarations

ETHICS APPROVAL AND CONSENT TO PARTICIPATE

The investigation conformed to the principles outlined in the Declaration of Helsinki.

hESCs, SA01 (Cellartis AB, Sweden) and H1 (WiCell Research Institute, USA), were provided by the INSERM cell bank « *ESteam Paris Sud - Plate-forme cellules souches* » (INSERM U935) according to the agreement n° RE14_007R of the French Biomedical Agency. The animal experiments herein presented were performed in compliance with relevant guidelines (European directive 2010/63/EU) and with the ethical approval of the Ethical Committee C2EA-26 *"Comité d'éthique en expérimentation animale de l'IRCIV",* officially registered with the French ministry of research. The ischemic tissue injury model in a mouse dorsal skinfold chamber (*agreement E-94-076-11)* and the hematopoietic reconstitution (*agreement* A94076030) were officially authorized by the French ministry of research (authorization number: 20570-2019050911277453v2 and 18028_2016100416362036v5, respectively), as per Directive 010/63 prescriptions and transposition into French law and regulations. Human embryos (range 7–8 weeks of gestation) were obtained following voluntary abortions. Tissue collection and use were performed according to the guidelines and with the approval of the French National Ethics Committee (French Biomedical Agency authorization No. PFS10_011). Informed consent was obtained from all donors of tissues. Written consent to the use of the tissues in research was obtained from all patients in accordance with the Declaration of Helsinki. Generated and analyzed data sets during the current study are available in GEO (accession number GSE194372) and can be queried at via the following link [https://www.ncbi.nlm.nih.gov/geo/query/acc.cgi?acc=GSE194372].

CONSENT FOR PUBLICATION

Not applicable

AVAILABILITY OF DATA AND MATERIALS

All materials are available by the corresponding author: alejandra.vargas@uclouvain.be

COMPETING INTERESTS

The authors declare no competing interests in relation to this study

FUNDING

This work was funded by INSERM, *Societé Française d'Hématologie* and the RHU program *"iLite"* on *"Innovations for Liver Tissue Engineering"* granted by PAI2 through ANR-16-RHUS-005.

AUTHOR CONTRIBUTIONS

A.V.V., M.T.M.G. and H.G. conceived and performed experiments. A.V.V wrote the manuscript. G.U., M.T.M.G. and H.G. secured funding, corrected the manuscript, provided expertise and feedback. A.C.P. performed the immunofluorescence experiments in the mouse dorsal chamber model. E.O. isolated

human EL sample, performed transcriptomic analyses and corrected the manuscript. M.L.G. and S.J. performed transcriptomic analyses. D.C. provided expertise on flow cytometry and performed cell sorting experiments. A.V.V., H.G., T.M., K.S. and V.R. conceived, performed, and analyzed in vivo experiments of endothelial cells. A.V.V., C.Q., M.T.M.G. and F.L. conceived, performed, and analyzed *in vivo* hematopoietic reconstitution.

ACKNOWLEDGEMENTS

We thank Dr. Anne Dubart-Kupperschmitt for kindly supply the hiPSC line A29 and to Dr. Antonietta Messina for her advice in immunofluorescence experiments. The authors greatly acknowledge Dr. Helene Berseneff as well as the orthogeny center staff for providing human embryo from voluntary abortions (Obstetrics and Gynecology Department, Rene Dubos Hospital, Pontoise, France). We thank Florian Beghi for his assistance to the *in vivo* hematopoietic reconstitution experiments and Nassim Arouche for his help in maintenance of hPSC lines. We also thank to Philippe Duquesnoy for his assistance in the design of RTqPCR experiments. We thank equally to Dr. Corine Laplace, head of the platform of imaging and cytometry at the Institute Gustave Roussy. We thank Robin Van Havermaet for his comments that greatly improved the manuscript.

References

1. Thomson JA, Itskovitz-Eldor J, Shapiro SS, Waknitz MA, Swiergiel JJ, Marshall VS, et al. Embryonic stem cell lines derived from human blastocysts. Science. 1998;282(5391):1145–7.
2. Takahashi K, Tanabe K, Ohnuki M, Narita M, Ichisaka T, Tomoda K, et al. Induction of Pluripotent Stem Cells from Adult Human Fibroblasts by Defined Factors. Cell. 2007;131(5):861–72.
3. Yu J, Vodyanik MA, Smuga-Otto K, Antosiewicz-Bourget J, Frane JL, Tian S, et al. Induced Pluripotent Stem Cell Lines Derived from Human Somatic Cells. Science. 2007 Dec 21;318(5858):1917.
4. Weijts B, Yvernogeau L, Robin C. Recent Advances in Developmental Hematopoiesis: Diving Deeper With New Technologies. Vol. 12, Frontiers in Immunology. Frontiers Media S.A.; 2021.
5. Garcia-Alegria E, Menegatti S, Fadlullah MZH, Menendez P, Lacaud G, Kouskoff V. Early Human Hemogenic Endothelium Generates Primitive and Definitive Hematopoiesis In Vitro. Stem Cell Reports. 2018 Nov 13;11(5):1061–74.
6. Dejana E, Hirschi KK, Simons M. The molecular basis of endothelial cell plasticity. Nat Commun. 2017;8(1):14361.
7. Tavian M, Hallais MF, Peault B. Emergence of intraembryonic hematopoietic precursors in the pre-liver human embryo. Development. 1999 Feb 15;126(4):793 LP – 803.
8. Oberlin E, Tavian M, Blazsek I, Péault B. Blood-forming potential of vascular endothelium in the human embryo. Development. 2002 Sep 1;129(17):4147 LP – 4157.
9. Taoudi S, Gonneau C, Moore K, Sheridan JM, Blackburn CC, Taylor E, et al. Extensive hematopoietic stem cell generation in the AGM region via maturation of VE-Cadherin + CD45 + pre-definitive HSCs.

Cell Stem Cell. 2008 Jul 3;3(1):99–108.

10. Ivanovs A, Rybtsov S, Anderson RA, Turner ML, Medvinsky A. Identification of the niche and phenotype of the first human hematopoietic stem cells. Stem cell reports. 2014 Mar 27;2(4):449–56.
11. Rybtsov S, Sobiesiak M, Taoudi S, Souilhol C, Senserrich J, Liakhovitskaia A, et al. Hierarchical organization and early hematopoietic specification of the developing HSC lineage in the AGM region. J Exp Med. 2011 Jun;6(6):1305–15. 208(.
12. Rybtsov S, Batsivari A, Bilotkach K, Paruzina D, Senserrich J, Nerushev O, et al. Tracing the Origin of the HSC Hierarchy Reveals an SCF-Dependent, IL-3-Independent CD43; Embryonic Precursor. Stem Cell Reports. 2014 Sep;9(3):489–501. 3(.
13. Nishikawa S, Nishikawa S, Hirashima M, Matsuyoshi N. Progressive lineage analysis by cell sorting and culture identifies FLK1 + VE- cadherin + cells at a diverging point of endothelial and hemopoietic lineages. 1998;1757:1747–57.
14. Oberlin E, Fleury M, Clay D, Petit-Cocault L, Candelier JJ, Mennesson B, et al. VE-cadherin expression allows identification of a new class of hematopoietic stem cells within human embryonic liver. Blood. 2010 Nov 25;116(22):4444–55.
15. Oberlin E, Hafny B, El, Petit-Cocault L, Souyri M. Definitive human and mouse hematopoiesis originates from the embryonic endothelium: A new class of HSCs based on VE-cadherin expression. Int J Dev Biol. 2010;54(6–7):1165–73.
16. Zhang Y, Clay D, Mitjavila-Garcia MT, Alama A, Mennesson B, Berseneff H, et al. VE-Cadherin and ACE Co-Expression Marks Highly Proliferative Hematopoietic Stem Cells in Human Embryonic Liver. Stem Cells Dev. 2018 Nov 14;28(3):165–85.
17. Kenswil KJG, Jaramillo AC, Ping Z, Chen S, Hoogenboezem RM, Mylona MA, et al. Characterization of Endothelial Cells Associated with Hematopoietic Niche Formation in Humans Identifies IL-33 As an Anabolic Factor. Cell Rep. 2018 Jan 16;22(3):666–78.
18. Ditadi A, Sturgeon CM, Keller G. A view of human haematopoietic development from the Petri dish. Nat Rev Mol Cell Biol. 2017;18(1):56–67.
19. Luo J, Shi X, Lin Y, Yuan Y, Kural MH, Wang J, et al. Efficient Differentiation of Human Induced Pluripotent Stem Cells into Endothelial Cells under Xenogeneic-free Conditions for Vascular Tissue Engineering. Acta Biomater. 2021 Jan;1:119:184–96.
20. Lin Y, Gil CH, Yoder MC. Differentiation, evaluation, and application of human induced pluripotent stem cell?derived endothelial cells [Internet]. Vol. 37, Arteriosclerosis, Thrombosis, and Vascular Biology. Lippincott Williams and Wilkins; 2017. pp. 2014–25.
21. Garcia-Alegria E, Potts B, Menegatti S, Kouskoff V. In vitro differentiation of human embryonic stem cells to hemogenic endothelium and blood progenitors via embryoid body formation. STAR Protoc. 2021 Mar 19;2(1).
22. Mora-Roldan GA, Ramirez-Ramirez D, Pelayo R, Gazarian K. Assessment of the hematopoietic differentiation potential of human pluripotent stem cells in 2d and 3d culture systems. Cells. 2021 Nov 1;10(11).

23. Philonenko ES, Tan Y, Wang C, Zhang B, Shah Z, Zhang J, et al. Recapitulative haematopoietic development of human pluripotent stem cells in the absence of exogenous haematopoietic cytokines. J Cell Mol Med. 2021 Sep 1;25(18):8701–14.
24. Oguro H. Generation of Hematopoietic Stem and Progenitor Cells from Human Pluripotent Stem Cells. In: Methods in Molecular Biology. Humana Press Inc.; 2019. pp. 245–57.
25. Hansen M, von Lindern M, van den Akker E, Varga E. Human-induced pluripotent stem cell-derived blood products: state of the art and future directions. Vol. 593, FEBS Letters. Wiley Blackwell; 2019. pp. 3288–303.
26. Sugimura R, Jha DK, Han A, Soria-Valles C, Da Rocha EL, Lu YF, et al. Haematopoietic stem and progenitor cells from human pluripotent stem cells. Nature. 2017 May 25;545(7655):432–8.
27. Chen T, Wang F, Wu M, Wang ZZ. Development of hematopoietic stem and progenitor cells from human pluripotent stem cells. J Cell Biochem. 2015 Jul 1;116(7):1179–89.
28. Prasain N, Lee MR, Vemula S, Meador JL, Yoshimoto M, Ferkowicz MJ, et al. Differentiation of human pluripotent stem cells to cells similar to cord-blood endothelial colony-forming cells. Nat Biotechnol. 2014;32(11):1151–7.
29. Nelson EA, Qiu J, Chavkin NW, Hirschi KK. Directed differentiation of hemogenic endothelial cells from human pluripotent stem cells. J Vis Exp. 2021 Mar 1;2021(169).
30. Ikuno T, Masumoto H, Yamamizu K, Yoshioka M, Minakata K, Ikeda T, et al. Efficient and robust differentiation of endothelial cells from human induced pluripotent stem cells via lineage control with VEGF and cyclic AMP. PLoS One. 2017 Mar 1;12(3).
31. Liu X, Qi J, Xu X, Zeisberg M, Guan K, Zeisberg EM. Differentiation of functional endothelial cells from human induced pluripotent stem cells: A novel, highly efficient and cost effective method. Differentiation. 2016 Oct 1;92(4):225–36.
32. Bertucci T, Kakarla S, Kim D, Dai G. Differentiating Human Pluripotent Stem Cells to Vascular Endothelial Cells for Regenerative Medicine, Tissue Engineering, and Disease Modeling. In: Methods in Molecular Biology. Humana Press Inc.; 2022. pp. 1–12.
33. Christensen K, Roudnicky F, Burcin M, Patsch C. Monolayer generation of vascular endothelial cells from human pluripotent stem cells. In: Methods in Molecular Biology. Humana Press Inc.; 2019. pp. 17–29.
34. Lee SJ, Kim KH, Yoon Y sup. Generation of Human Pluripotent Stem Cell-derived Endothelial Cells and Their Therapeutic Utility. Vol. 20, Current Cardiology Reports. Current Medicine Group LLC 1; 2018.
35. Zhang F, Zhu Y, Chen J, Kuang W, Huang R, Duan F, et al. Efficient endothelial and smooth muscle cell differentiation from human pluripotent stem cells through a simplified insulin-free culture system. Biomaterials. 2021 Apr 1;271:120713.
36. Choi K-D, Yu J, Smuga-Otto K, Salvagiotto G, Rehrauer W, Vodyanik M, et al. Hematopoietic and Endothelial Differentiation of Human Induced Pluripotent Stem Cells. Stem Cells. 2009 Mar;27(3):559–67.

37. Netsrithong R, Suwanpitak S, Boonkaew B, Trakarnsanga K, Chang LJ, Tipgomut C, et al. Multilineage differentiation potential of hematoendothelial progenitors derived from human induced pluripotent stem cells. Stem Cell Res Ther. 2020 Dec 1;11(1).
38. Lange L, Morgan M, Schambach A. The hemogenic endothelium: a critical source for the generation of PSC-derived hematopoietic stem and progenitor cells. Vol. 78, Cellular and Molecular Life Sciences. Springer Science and Business Media Deutschland GmbH; 2021. p. 4143–60. Available from: https://pubmed.ncbi.nlm.nih.gov/33559689/.
39. Ditadi A, Sturgeon CM. Directed differentiation of definitive hemogenic endothelium and hematopoietic progenitors from human pluripotent stem cells. Methods. 2016 May 15;101:65–72.
40. Galat Y, Dambaeva S, Elcheva I, Khanolkar A, Beaman K, Iannaccone PM, et al. Cytokine-free directed differentiation of human pluripotent stem cells efficiently produces hemogenic endothelium with lymphoid potential. Stem Cell Res Ther. 2017 Mar;17(1):1–11. 8(.
41. Steichen C, Luce E, Maluenda J, Tosca L, Moreno-Gimeno I, Desterke C, et al. Messenger RNA- Versus Retrovirus-Based Induced Pluripotent Stem Cell Reprogramming Strategies: Analysis of Genomic Integrity. Stem Cells Transl Med. 2014 Jun;3(6)(1):686–91.
42. Guillevic O, Ferratge S, Pascaud J, Driancourt C, Boyer-Di-Ponio J, Uzan G. A Novel Molecular and Functional Stemness Signature Assessing Human Cord Blood-Derived Endothelial Progenitor Cell Immaturity. PLoS One. 2016 Jan 4 [cited 2016 Apr 22];11(4):e0152993.
43. Rouffiac V, Roux KS, Le, Salomé-Desnoulez S, Leguerney I, Ginefri JC, Sébrié C, et al. Multimodal imaging for tumour characterization from micro- to macroscopic level using a newly developed dorsal chamber designed for long-term follow-up. J Biophotonics. 2020 Jan 1;13(1).
44. Sato Y, Nakajima S, Shiraga N, Atsumi H, Yoshida S, Koller T, et al. Three-dimensional multi-scale line filter for segmentation and visualization of curvilinear structures in medical images. Med Image Anal. 1998;2(2):143–68.
45. Arganda-Carreras I, Fernández-González R, Muñoz-Barrutia A, Ortiz-De-Solorzano C. 3D reconstruction of histological sections: Application to mammary gland tissue. Microsc Res Tech. 2010 Oct;73(11)(1):1019–29.
46. Féraud O, Valogne Y, Melkus MW, Zhang Y. Donor Dependent Variations in Hematopoietic Differentiation among Embryonic and Induced Pluripotent Stem Cell Lines. 2016;1–22.
47. Lu S-J, Feng Q, Caballero S, Chen Y, Moore M, Grant S. MB, et al. Generation of functional hemangioblasts from human embryonic stem cells. Nat Methods. 2007;4(6):501–9.
48. Shalaby F, Janet R, Yamaguchi TP, Gertsenstein M, Wu XF, Breitman ML, et al. Failure of blood-island formation and vasculogenesis in Flk-1-deficient mice. Vol. 376: Nature. Nature Publishing Group; 1995 Jul.
49. Lanner F, Sohl M, Farnebo F. Functional arterial and venous fate is determined by graded VEGF signaling and notch status during embryonic stem cell differentiation. Arterioscler Thromb Vasc Biol. 2007 Mar 1;27(3):487–93.

50. Sturgeon CM, Ditadi A, Awong G, Kennedy M, Keller G. Wnt signaling controls the specification of definitive and primitive hematopoiesis from human pluripotent stem cells. 2014;(May).
51. Ditadi A, Sturgeon CM, Tober J, Awong G, Kennedy M, Yzaguirre AD, et al. Human definitive haemogenic endothelium and arterial vascular endothelium represent distinct lineages. Nat Cell Biol. 2015 May 5 [cited 2020 Oct 3];17(5):580–91.
52. Lian X, Bao X, Al-Ahmad A, Liu J, Wu Y, Dong W, et al. Efficient Differentiation of Human Pluripotent Stem Cells to Endothelial Progenitors via Small-Molecule Activation of WNT Signaling. Stem Cell Reports. 2014 Nov;11(5):804–16. 3(.
53. Sahara M, Hansson EM, Wernet O, Lui KO, Später D, Chien KR. Manipulation of a VEGF-Notch signaling circuit drives formation of functional vascular endothelial progenitors from human pluripotent stem cells. Cell Res. 2014 May 9;24:820.
54. Nafria M, Bonifer C, Stanley EG, Ng ES, Elefanty AG. Protocol for the Generation of Definitive Hematopoietic Progenitors from Human Pluripotent Stem Cells. STAR Protoc. 2020;1(3):100130.
55. Kennedy M, D'Souza SL, Lynch-Kattman M, Schwantz S, Keller G. Development of the hemangioblast defines the onset of hematopoiesis in human ES cell differentiation cultures. Blood. 2007;109(7):2679–87.
56. Zambidis ET, Park TS, Yu W, Tam a, Levine M, Yuan X, et al. Expression of ACE (CD143) identifies and regulates primitive hemangioblasts derived from human pluripotent stem cells. Blood. 2008;112(9):3601–15.
57. Proust R, Ponsen AC, Rouffiac V, Schenowitz C, Montespan F, Ser-Le Roux K, et al. Cord blood-endothelial colony forming cells are immunotolerated and participate at post-ischemic angiogenesis in an original dorsal chamber immunocompetent mouse model. Stem Cell Res Ther. 2020 May 7;11(1):172.
58. Gori JL, Butler JM, Chan YY, Chandrasekaran D, Poulos MG, Ginsberg M, et al. Vascular niche promotes hematopoietic multipotent progenitor formation from pluripotent stem cells. J Clin Invest. 2015 Mar 2;125(3):1243–54.
59. Ledran MH, Krassowska A, Armstrong L, Dimmick I, Renström J, Lang R, et al. Efficient hematopoietic differentiation of human embryonic stem cells on stromal cells derived from hematopoietic niches. Cell Stem Cell. 2008 Jul 3;3(1):85–98.
60. Tavian M, Coulombel L, Luton D, Clemente HS, Dieterlen-Lièvre F, Péault B. Aorta-associated CD34 + hematopoietic cells in the early human embryo. Blood. 1996 Jan 1;87(1):67–72.
61. Féraud O, Valogne Y, Melkus MW, Zhang Y, Oudrhiri N, Haddad R, et al Donor Dependent Variations in Hematopoietic Differentiation among Embryonic and Induced Pluripotent Stem Cell Lines. Kaufman D, editor. PLoS One. 2016 Mar 3;11(3):e0149291.
62. Jahan B, McCloskey KE. Differentiation and expansion of endothelial cells requires pre-optimization of KDR + expression kinetics. Stem Cell Res. 2020 Jan 1;42:101685.
63. Osafune K, Caron L, Borowiak M, Martinez RJ, Fitz-Gerald CS, Sato Y, et al. Marked differences in differentiation propensity among human embryonic stem cell lines. Nat Biotechnol. 2008

Mar;26(3):313–5.

64. Lancrin C, Sroczynska P, Stephenson C, Allen T, Kouskoff V, Lacaud G. The haemangioblast generates haematopoietic cells through a haemogenic endothelium stage. Nature. 2009 Feb 12;457(7231):892–5.
65. Choi K, Kennedy M, Kazarov A, Papadimitriou JC, Keller G. A common precursor for hematopoietic and endothelial cells. Development. 1998 Feb 1;125(4):725–32.

Figures

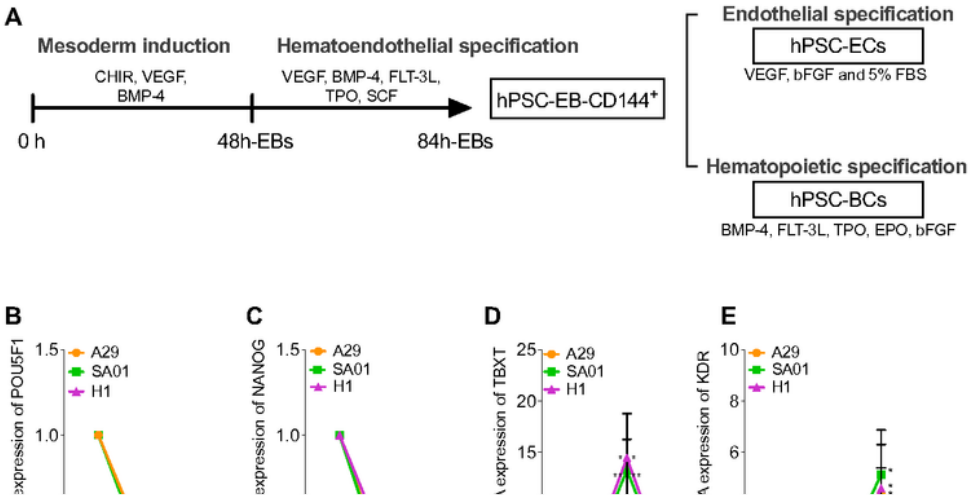

Figure 1

hPSC differentiation into a hematoendothelial population. **(A)** One hiPSC cell line (A29) and two hESC cell lines (SA01 and H1) were differentiated following embryoid body (EB) formation for 84 hours supplied with growth factors inducing mesoderm and hematoendothelial specification. $CD144^{+}$ sorted cells were differentiated into endothelial and hematopoietic lineage in the presence of specific growth factors. **(B-E)** EBs were analyzed at 48h and 84h by RTqPCR and compared to the hPSCs preceding EB formation (0h)

for the stem cell genes *POU5F1* **(B)** and *NANOG* **(C)**, the mesoderm gene *TBXT* **(D)** and the hematoendothelial gene *KDR* **(E)**. **(F)** At 84h, EBs were dissociated enzymatically and analyzed by flow cytometry for the expression of hematoendothelial (CD309, CD34 and CD143), endothelial (CD144 and CD31) and hematopoietic markers (CD43, CD41 and CD45), n=30 for every hPSC cell line and marker. **(G)** Representative flow cytometry analysis of CD143, CD309, CD34 and CD31 within the CD144+ population from 84h-EBs (see also supplementary figure 1). **(H-I)** 84h-EBs were sorted based on the expression of CD144 and analyzed for the expression of the hematoendothelial transcription factors *ETV2* (h) and *RUNX1* (I) by RTqPCR, n=5 independent experiments for each cell line. *P-value < 0.05; **P-value<0.005, ***P-value<0.0005. Data are represented as mean ± SEM.

Figure 2

Endothelial differentiation of hPSC-EB-CD144^{+}. (A) Representative phase-contrast images of endothelial colonies formed from single CD144^{+} cells at day 7 (left) and at day 15 (right). Scale bar 100 µm. **(B)** Confocal microscope images of endothelial colonies from the colony forming assay essay. hPSC-ECs were labeled against CD31 (green), CD144 (red) and with DAPI for the nuclei (blue). Scale bar 500 µm. **(C)** Representative phase-contrast images of hPSC-derived endothelial cells (hPSC-ECs) from passage (p) 1

to 5 derived from CD144+-EBs. Scale bar 500 µm. **(D)** Endothelial phenotype was analyzed along the passages by flow cytometry for hPSC-EC from A29 (left), SA01 (center) and H1 (right) cell lines. hPSC-ECs derived from the three cell lines kept a stable phenotype characterized by the expression of CD309, CD144, CD31, CD34 and CD143. The expression of hematopoietic markers was negligeable at every passage. **(E)** Confocal microscope images of hPSC-ECs and Endothelial colony-forming cells (ECFCs) labeled with antibodies against von Willebrand Factor (vWF, red) and CD31 (green). Nuclei stained with DAPI (blue). Scale bar 500 µm. **(F)** Cumulative population doubling (CPD) indicates hPSC-ECs were highly proliferative during the first 10 days in culture. Differences among the proliferative rate were observed among the hPSC-cell lines being A29 the less proliferative. **(G-I)** RTqPCR analysis of arterial (*NRP1* and *EFNB2*), venous genes (*NRP2, EPHB4* and *COUPTFII*) and the pan-endothelial gene *CDH5* (CD144) in hPSC-ECs after treatment with an antagonist of Notch (DAPT) during the EC differentiation (see also supplementary figure 2), n=5 independent experiments for every cell line. *P-value<0.05; **P-value<0.005 and ***P-value<0.0005. Data are represented as mean ± SEM.

Figure 3

hPSC-EB-CD144$^+$ derived endothelial cells are functional *in vitro* and *in vivo*. (A) Confocal microscopy images of hPSC-ECs and ECFCs after 4 hours of incubation with acLDL-AlexaFluor-488. CD31 in red and nuclei in blue (DAPI). Scale bar 100 µm. **(B-B')** Endothelial activation by TNF-α assay. Expression of ICAM-1 in hPSC-ECs and ECFCs was analyzed by flow cytometry in the absence and presence of TNF-α **(B)**. High positive cells which were only detected after incubation with TNF-α **(B')**. (**C-C'**) Matrigel-based tube formation assay 8 hours after seeding **(C)**. Phase contrast images with scale bar 1000 µm C'. Cell network characterisation based on the number of segments, meshes, branches and nodes. **(D-D')** hPSC-ECs nitric oxide (NO) production was analyzed based on the expression of the endothelial nitric oxide synthase (eNOS) measured by flow cytometry **(D)**. In parallel, the probe DAF-FM diacetate was used to detect NO in hPSC-ECs and ECFCs. DAF-FM fluorescence was measured by flow cytometry in cells that were not incubated with the probe (-DAF-FM) as a negative control, in cells incubated with the probe alone (+DAF-FM) and in the presence of a S-nitrosothiol molecule (+DAF-FM +SNAP) or in cells previously stimulated with lipopolysaccharides (+DAF-FM +LPS), the two latter as positive controls, n=5 independent experiments for every cell line **(D')**. **(E)** Representative confocal image at day 19 post-injection of a mouse dorsal skinfold chamber with ischemia, injected with mcherry-hPSC-ECs. Vessel perfusion was observed thanks to the injection of dextran 70 kDa-FITC (green). Scale bar: 200 µm. **(F)** Percentage of new blood vessels formed at day 19 post-injection. n=6 independent experiments. **(G)** Confocal images of the dorsal chambers analyzed post-mortem by immunofluorescence. Yellow arrows indicate human CD144$^+$ ECs (green) localized at the wall of blood vessels. Scale bar: 100 µm. *P-value<0.05; **P-value<0.005 and ***P-value<0.0005. Data are represented as mean ± SEM.

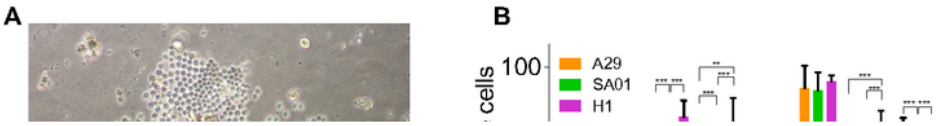

Figure 4

Differentiation of hPSC-EB-CD144^{+} into hPSC-BCs. (A) Phase contrast microscopy images of hPSC-derived blast colonies (hPSC-BCs). Scale bar 100 µm. **(B-C)** Flow cytometry analysis of day 6-hPSC-BCs for hematoendothelial (CD309, CD143 and CD34), endothelial (CD144 and CD31) and hematopoietic

markers (CD43, CD45 and CD41) as simple **(B)** and double labelling **(C)**, n=15 for every hPSC line and marker. **(D-H)** Expression of hematopoietic and endothelial transcription factors in $CD144^{+}$-EBs, hPSC-ECs and hPSC-BCs: *SCL* **(D)**, *GATA2* **(E)**, *RUNX1c* **(F)**, *GATA1* **(G)** and *HOXA3* **(H)**. Data are represented as mean ± SEM, n=5 independent experiment for each cell line. *P-value<0.05; **P-value<0.005 and ***P-value<0.0005.

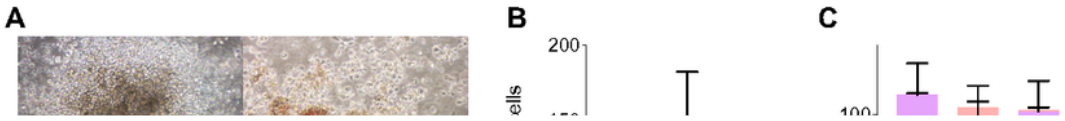

Figure 5

Functional characterization of hematopoiesis. (A) Phase contrast microscopy images of myeloid, CFU-GM (image above left) and CFU-GEMM (image above right), and erythroid colonies, BFU-E (image below left), derived from hPSC-BCs. Scale bar: 100 µm. **(B)** Number of hematopoietic colonies per 10^5 hPSC-BCs seeded cells in methylcellulose (A29 n=7, SA01 n=6 and H1 n= 10). **(C)** Percentage of every type of myeloid and erythroid colony per hPSC line. **(D)** Relative mRNA expression of the hemoglobin subunit epsilon-1 (HBE1), gamma-1 (HBG1) and beta-1 (HBB1) in the BFU-E and CFU-GEMM derived from every hPSC-cell line compared to mRNAs from human fetal liver. **(E)** Ratio of gamma/epsilon and epsilon/beta hemoglobin expression of the BFU-E and CFU-GEMM. **(F)** Presence of human DNA in the mouse BM was assessed by qPCR with primers amplifying specifically the human gene CD45. Data are represented as mean ± SEM. For the *in vivo* experiment: ND: non detected, n=2 for $CD34^+$ and PBS and n=5 for $CD144^+$-EBs. For all the other histograms: n=5 independent experiments for each cell line. *P-value<0.05; **P-value<0.005 and ***P-value<0.0005.

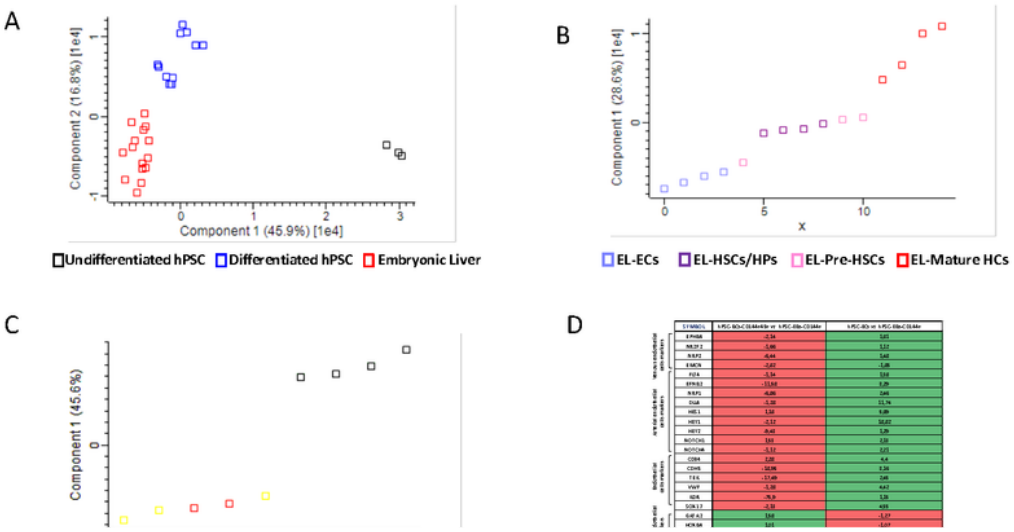

Figure 6

Transcriptomic Analyses. (A-C) PCA loading plot of the first two principal components distribution of EL (red), differentiated hPSC (blue) and undifferentiated hPSC (black) **(A)**. Distribution of EL-ECs (mauve), EL-HSCs/HPs (purple), EL-Pre-HSCs (pink) and EL-mature HCs (red) **(B)**. Distribution of hPSC-derived populations, hPSC-BCs (blue), hPSC-BC-CD144+CD45+ (grey), hPSC-EB-CD144^{+} (orange) and hPSC-ECs (yellow) **(C)**, each square represents one sorted cell population. **(D)** Visualizing significant differential

level expression of selected genes of hPSC-BC-CD144^{+}CD45^{+} and hPSC-ECs between hPSC-EB-CD144^{+} revealing distinct endothelial, hemogenic endothelial and hematopoietic signatures. All fold changes were calculated respect to the mean value of hPSC-EB-CD144^{+}. P-value ≤ 0.05. (**E-G**) GSEA curves for the most significantly enriched hematopoietic and endothelial GO biological process in hPSC-EB-CD144^{+} **(E)**, hPSC-ECs **(F)** and hPSC-BC-CD144+CD45^{+} **(G)** compared to undifferentiated hPSCs. Enrichment analysis was performed using Gene Set Enrichment Analysis software v4.1.0 and probing the c5.go.bp.v7.4 collection of the Molecular Signatures Database (MSigDB). GO=Gene Ontology; NES = normalized enrichment score. P-value ≤ 0.05. **(H)** Non-supervised hierarchical clustering of transcript (rows) and samples (colums) based on their distance using Pearson correlation. Color intensity indicates expression levels scaled to the column mean. The heatmap is coded red for increasing and green for decreasing. The colored bar on top indicates how the heat map colors are related to the standard score (z-score), i.e. the deviation from row mean in units of standard deviations above or below the mean. **(I)** Model summarizing transcriptomic results where hPSC-EB-CD144^{+} give rise to hPSC-ECs, hPSC-BCs and hPSC-BC-CD144^{+}CD45^{+}, these two latter containing primitive and definitive hematopoietic progenitors, respectively.

Supplementary Files

This is a list of supplementary files associated with this preprint. Click to download.

- SupplementarydataVargasValderramaA.docx